HPU2 Journal of Sciences:
Natural Sciences and Technology

Journal homepage: https://sj.hpu2.edu.vn

Article type: Research article

The origins of size-dependent UV stabilities of CdZnTeS alloyed quantum dots

Phuong-Nam Nguyen[a], Thi-Phuong Nguyen[b], Anh-Duc Vu[c], Duy-Khanh Nguyen[a], Duy-Tung Dao[d], Xuan-Dung Mai[a*]

[a]*Hanoi Pedagogical University 2, Vinh Phuc, Vietnam*
[b]*Hoang Hoa Tham Elementary and Secondary School, Bac Ninh, Vietnam*
[c]*Kazan National Research Technological University, Republic of Tatarstan, Russian*
[d]*Advanced Photonics Research Institute, Gwangju Institute of Science and Technology, Gwangju, Republic of Korea*

Abstract

CdTe-based quantum dots (QDs) have been used as active materials in various applications, such as sensing, imaging, and light-harvesting devices where the QDs are continuously illuminated by suitable lights. Passivation of CdTe QDs with stable inorganic layers to form core/shell or core/multiple-shell structures has been demonstrated to improve the stabilities of QDs against illumination. However, information related to the UV stability of newly developed CdZnTeS alloyed QDs has not been fully explored yet. Herein, we synthesized CdZnTeS alloyed QDs of different sizes and compared their size-dependent stabilities under UV irradiation. Upon UV exposure the first excitonic peak of QDs blue-shifted, gradually and the relative Cd concentration decreased indicating that QDs were steadily dissolved. We found that the smaller QDs dissolved faster than the larger QDs. By correlating this with the change in the QDs' crystalline structure corroborated by X-ray diffraction studies, we demonstrated that the alloyed structure with a sulfide-rich surface enhances the stabilities of larger QDs. The size-dependent stabilities of alloyed QDs demonstrated here provide information for selecting the right QDs for specific applications.

Keywords: CdTe quantum dots, alloyed structure, size-dependent, stabilities, dissolution

1. Introduction

Water-soluble CdTe QDs have been demonstrated to be applicable in many applications including (but not limited to) light-harvesting materials in solar cells [1], [2], photoluminescence-based sensing [3], [4], and bioimaging [5], [6]. In solar cell applications, the QDs' size determines the

* Corresponding author, E-mail: xdmai@hpu2.edu.vn

https://doi.org/10.56764/hpu2.jos.2024.3.1.39-46

Received date: 17-01-2024 ; Revised date: 06-02-2024 ; Accepted date: 04-03-2024

portion of the solar spectrum to be absorbed because of size-dependent QDs' bandgap [1], [7]. The size of QDs also influences the band-edge energy levels that strongly affect the efficiency of electron-hole pair separation at the QDs interfaces [1], [8]. In photoluminescence-based sensing applications, the PL intensity of CdTe QDs is changed functionally with the concentration of analyte [9]–[11]. The variation in PL intensity could be due to the loss of capping ligands [12], charge transferring at QD-analyst interfaces [13], and the interaction between the analyst and QDs' surface [14]. Nevertheless, the response of PL intensity relate to the surfaces of QDs which is also influenced by the QDs' size [2], [15], [16]. Therefore, any variation in the QDs' size upon light illumination, the most common working condition of QDs, could lead to failures in application.

Under excitation, especially in the presence of oxygen, CdX (X=S, Se, Te) QDs are oxidized gradually leading to a number of effects including a decrease in PL efficiency and liberation of toxic Cd^{2+} ions [17], [18]. Coating CdTe QDs with stable inorganic shells, such as CdS and ZnS shells in either a core/shell or a core/multiple-shell structure has been widely used to enhance the PL efficiency and to reduce the leaching of Cd ions [19], [20]. One drawback of the core/shell structures is time-consuming syntheses which include the preparation of CdTe QDs and post-growing shells [21], [22]. Alternatively, a one-pot procedure in which an alkaline mixture of Cd^{2+}, Zn^{2+}, Te^{2-} precursor (Te or Na_2TeO_3), and $NaBH_4$ is heated in the presence of mercapto ligands has been developed to prepare CdZnTeS alloyed QDs [23], [24]. The alloyed structure with a ZnS-rich surface makes CdZnTeS QDs to be highly photoluminescent. To utilize those alloyed QDs into practical applications, some important information such as the emission yield [25], toxicity [26], redox potential [27], and size-dependent reactivity [14], [28] have been explored. However, information related to the stabilities of alloyed QDs under excitation conditions has not been fully described yet.

In this study, we synthesized CdZnTeS alloyed QDs of different sizes and correlated the size of QDs to their pH and UV stability. Optical characterizations and the cadmium analysis revealed that the smaller QDs are more prone to dissolve than the bigger QDs. The results presented in this study offer further insights into the properties of CdZnTeS alloyed QDs relevant to practical applications.

2. Experimental

2.1. The synthesis and purification of CdZnTeS alloyed quantum dots

CdZnTeS alloyed QDs were synthesized by adopting a procedure reported previously [14]. Briefly, a mixture containing 0.9 mmol $CdCl_2$, 0.1 mmol $ZnCl_2$, 1.24 mmol GSH, 0.18 mmol Na_2TeO_3, and 1.98 mmol $NaBH_4$ at a pH of 10.5 (adjusted by a NaOH 1.0 M solution) was refluxed in an Ar-filled flask. QDs of different sizes whose first excitonic peaks at 477 nm (denoted as g-QDs), 522 nm (y-QDs), and 664 nm (r-QDs) were obtained after 10 minutes, 60 minutes, and 180 minutes of refluxing, respectively. The crude QDs were washed by precipitation with acetone (Aladdin chemicals, HPLC grade), centrifuged at a speed of 5000 rounds per minute for 6 minutes, and re-dispersed in water. The precipitation – centrifugation – dispersion cycle was repeated twice to obtain pure QDs which were stored in black vials at 4^{o}C for further use.

2.2. Characterizations

A JEM 2100 microscope was used to conduct TEM images while A D8 Advance X-ray diffractometer was used to measure X-ray diffraction (XRD) of QDs. To study the UV stability of QDs, aqueous solutions of QDs in quartz flasks were stirred and placed in a chamber (55×35×40 cm). The UV light source was 365 nm LEDs with a total power of 10 W and the distance from LEDs to the

flasks was 10 cm. Aliquots were taken after different periods of UV exposure for optical characterizations. The absorption spectra were conducted on a UV-2450 (Shimadzu) spectrophotometer and the photoluminescent spectra were measured on an FLS1000 (Edinburgh) spectrometer. For elemental analysis, the QDs solutions obtained after different periods (0, 30, 60, and 180 minutes) of UV exposure were sequentially filtered via 0.21 μM syringe filters, precipitated with excess acetone, and centrifuged at 10.000 rounds per minute for 10 minutes to obtain QDs solids. The QDs solids were digested by 25 ml of nitric acid solution (2% by weight) at 50°C for 2 hours and diluted to 100 ml for quantitative analysis of Cd^{2+} concentration which was conducted on an inductively coupled plasma mass spectrometry (Agilent 7900). The concentrations of Cd^{2+} in each set of QDs' size was normalized to the 0-minute aliquot.

3. Results and discussion

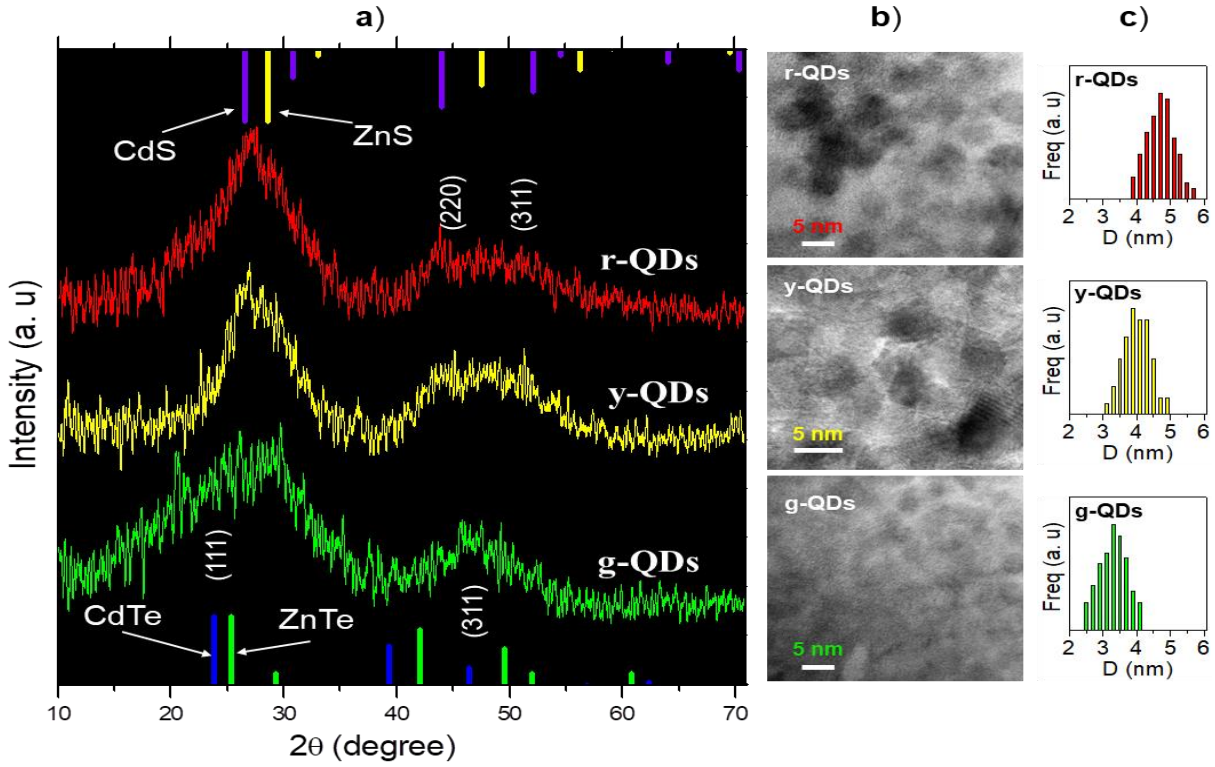

Figure 1. (a) XRD patterns, (b) TEM images, and (c) size-distribution of green emitting (g-QDs), yellow-emitting (y-QDs), and red-emitting (r-QDs) CdZnTeS alloyed quantum dots. In (a) the standard XRD database of CdTe (JCPDS#: 15-0770), ZnTe (JCPDS#: 15-0746), CdS (JCPDS#: 47-1179), and ZnS (JCPDS#: 05-0566) crystals are shown for referring.

XRD patterns of QDs are shown in Figure 1a in comparison with other possible crystal phases including zinc-blende CdTe, ZnTe, CdS, and ZnS. In g-QDs, a clear diffraction peak positioned at 46.4° could be assigned to the (311) plane of CdTe (Joint Committee on Powder Diffraction Standards, JPCDS, file number 15-0770) [22]. The diffraction peak from (111) planes of CdTe at 23.8° was broadened, probably due to the inclusion of Zn^{2+} and S^{2-} ions into the CdTe crystal and due to the small size of g-QDs. The diffraction peak at 46.4° observed in g-QDs likely evolved into two peaks at about 44° and 50.7° which are close to the diffraction positions of (220) and (311) planes of ZnTe and CdS [24]. Additionally, the diffraction peak positioned at about 27° became sharper in y-, and r-QDs; the peak was in the between diffraction positions (111) of CdS and ZnS. TEM images of QDs shown

in Figure 1b clearly exhibit individual spherical crystals. The diameter of g-, y-, and r-QDs shown in Figure 1c were about 3.4, 4.1, and 4.8 nm, respectively. Based on TEM images and XRD patterns of QDs shown in Figure 1 we deduced that g-QDs were mostly CdTe nanocrystals. As the QDs grew Cd^{2+}, Zn^{2+}, Te^{2-}, and S^{2-} ions assembled gradually into the alloyed crystals of CdZnTeS QDs.

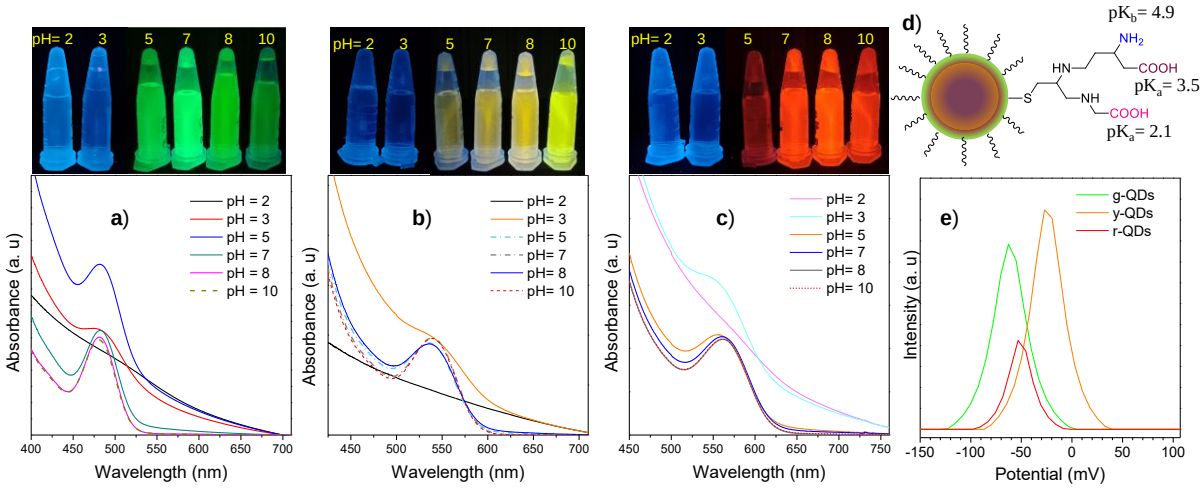

Figure 2. Absorption spectra measured at different pH of (a) g-QDs, (b) y-QDs, and (c) r-QDs. The pictures inserted above each graph are the QDs solutions under UV lamp (365 nm). d) Model of GSH capped quantum dots. (e) Zeta potential of quantum dots measured at pH of 7.

Water solubility is one of the major characteristics targeted for the applications of CdTe-based QDs. In some applications, such as heavy metal ion sensing [12], [29], [30], the effects of pH on QDs are important because pH determines the type of metal ions and their relative concentrations in water [31]. We measured the absorption spectra at different pH levels to study the effects of pH on the colloidal stability of CdZnTeS alloyed QDs, and the results are shown in Figure 2. In neutral or slightly alkaline pH, the absorption spectra of QDs exhibit well-resolved excitonic peaks at 477 nm (g-QDs), 522 nm (y-QDs), or 664 nm (r-QDs). The QDs solutions emit intensively under UV light (365 nm) as seen in the insets in Figure 2a-c. At pH of 5, QDs were partially accumulated forming larger aggregates that enhance light loss due to light-scattering effects as indicated by an increase in the absorbance as clearly seen in Figure 2a. At lower pH, the excitonic peaks were blurred and the QDs solutions did not exhibit fluorescence indicating that all QDs were precipitated. Those results suggest that g-QDs were colloidally stable at pH $\geqslant$7 while y-, and r-QDs were stable at pH $\geqslant$5.

It has been demonstrated that GSH cap onto the surface of CdZnTeS alloyed QDs via Cd-S bonds and that GSH ligands expose outward two –COOH groups and one $–NH_2$ group whose pK_a values are 2.1, 3.5, and 9.1, as respectively indicated in Figure 2d, [14], [26]. At neutral pH the carboxyl groups are in a carboxylate ($–COO^-$) state while the amino groups are in a protonated ($–NH_3^+$) state making the surface of QDs negative, as proved by Zetal potential measurements shown in Figure 2e. By using the pKa values we can calculate that at pH of 3 the total concentration of $–COO^-$ equals to that of $–NH_3^+$ so that the surface charge of QDs is neutral. This theoretical calculation explained why the QDs were precipitated when pH was about 3 as mentioned above.

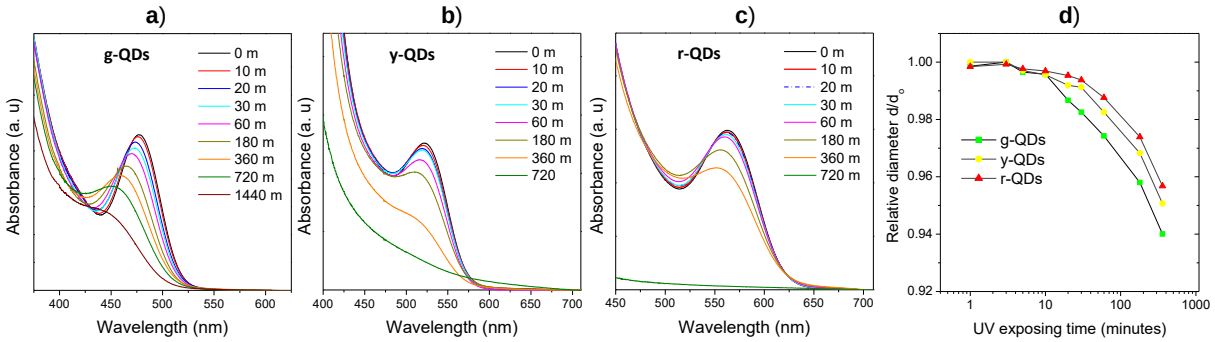

Figure 3. (a)-(c) Absorption spectra of green emitting (g-QDs), yellow-emitting (y-QDs), and red-emitting (r-QDs) CdZnTeS alloyed quantum dots. (d) Calculated relative diameter (d/d_o) of quantum dots using the position of first excitonic peak in (a)-(c).

Table 1. Relative concentration of Cd digested from quantum dots after UV exposure.

UV exposing time (*minutes*)	**Relative concentration**		
	g-QDs	**y-QD**	**r-QDs**
0	1	1	1
30	0.95	0.97	0.98
60	0.91	0.94	0.96
180	0.86	0.92	0.92

The effects of UV exposure on the absorption and emission properties of QDs are shown in Figure 3. As the exposure time increased, the first excitonic peaks of all QDs blue-shifted and became blurred. After about 720 minutes y- and r-QDs were precipitated as indicated by the scattering-like absorption feature in Figure 3b-c. We calculated the bandgap (E_o) from the position of the first excitonic peak and used a correlation function (1) to determine the diameter (d) of QDs at different periods of UV irradiation.

$$E_o = 1.51 + \frac{1}{0.048d^2 + 0.29d - 0.09} \quad (1)$$

In (1), 1.51 is the band gap of bulk CdTe [7]. The variation of the relative diameter (d/d_o) of QDs with UV irradiation is summarized in Figure 3d. Obviously, the relative diameter of the smaller QDs decreased more quickly than the larger ones. To correlate the decrement in the size of QDs to a possible release of toxic Cd ions, we precipitated QDs and analyzed the amount of remaining Cd using an ICP-MS method (see the experimental section). The relative concentration of Cd decreased faster in the smaller QDs. This trend was in line with the decreasing QDs' size discussed in Figure 3d indicating that UV exposure induces the dissolution of QDs into ionic species. Under UV irradiation, the smaller QDs were dissolved more rapidly than the larger QDs.

In a previous study [14] we demonstrated that UV irradiation causes the PL efficiency of the smaller QDs to decrease faster than the bigger QDs. The PL decrease induced by UV exposure has been reported widely, known as photobleaching, and is usually attributed to the oxidation of the QDs surfaces [18]. The oxidation of surficial Te^{2-} ions leads to the gradual detachments of Te^{2-} (in the forms of oxygen-containing anions) and Cd^{2+} ions. Those detachments cause several effects including (1) The size of QDs decreases as directly indicated by the fist excitonic peaks shifting to lower wavelength (Figure 3); (2) The leaching of Cd^{2+} ions, as discussed in Table 1, that causes potential toxicity of QDs; (3) The detachment of Cd^{2+} ions also takes GSH capping molecules out of the QDs' surface resulting in decreased colloidal stability as indicated by the precipitation of QDs after 720 minutes of UV exposure (Figure 3b-c); and (4) The oxidation of Te^{2-} ions and the consequent ions

detachments leaves more defects on the surface of QDs that reduce the emission efficiency of QDs. To explain the effects of size on the UV stability of QDs we put a tentative model in Figure 4. The model is advised from the XRD results (Figure 1a) and related discussion that more Zn^{2+} and S^{2-} ions were incorporated in the bigger QDs.

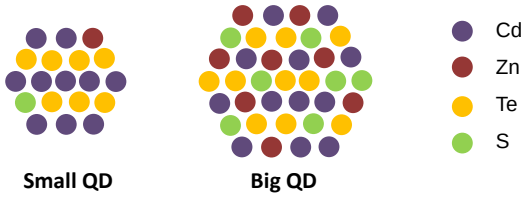

Figure 4. Quantum dot model represent the effects of size on the incorporation of Zn^{2+} and S^{2-} ions into the crystalline structure.

Table 2. The dissociation energy of interested bonds in quantum dots.

Bond	**Energy (*kJ/mol*)**
Cd-Te	100.0±15.2
Zn-Te	117.6±18.0
Cd-S	208.5±20.9
Zn-S	224.8±12.6

Since S^{2-} ions were in-situ formed in the reaction solution via the thermal decomposition of GSH ligands it is reasonable that S^{2-} ions were likely deposited on the surface of growing QDs. The presence of S^{2-} ions stabilized the QDs crystalline because the bond dissociation energy of Cd-S (208.5±20.9 kJ/mol) is much higher than that of CdTe (100±15.2 kJ/mol), Table 2 [32]. Additionally, the incorporation of Zn^{2+} ions also stabilized QDs because Zn-X (X=S, Te) bonds are more stable than corresponding Cd-X bonds. Likely, the alloyed structure with an S^{2-}–rich surface enhances the UV stability of QDs, especially bigger QDs.

4. Conclusion

The pH and UV stability of highly photoluminescent, one-pot-synthesized CdZnTeS quantum dots have been examined to clarify their potential applications. Depending on pH, carboxyl and amino groups on the surfaces of QDs are either in acidic or basic states accounting for the Zeta potential of QDs that makes QDs colloidal stable in neutral or alkaline media. Comparing the crystalline structure and UV stabilities of QDs of different sizes revealed that as the QDs' size increases the structure becomes alloyed with an S-rich surface and the UV-induced dissolution rate decreases. The presence of Zn^{2+} and S^{2-} ions enhances the crystalline stability of QDs which makes the bigger QDs more UV stable than the smaller QDs. Nevertheless, the alloyed QDs of all sizes dissolve gradually upon UV irradiation giving rise to a potential release of toxic Cd ions. The results demonstrated herein suggest strategies to increase the stability of CdZnTeS alloyed QDs, hence reducing the toxicity of QDs, by depositing additional S^{2-} and Zn^{2+} ions.

Acknowledgement

This study was supported by Hanoi Pedagogical University 2 via project number SV.2023.HPU2.04.

References

[1] E. Elibol, "Quantum dot sensitized solar cell design with surface passivized CdSeTe QDs," *Sol. Energy*, vol. 206, pp. 741–750, Aug. 2020, doi: 10.1016/j.solener.2020.06.002.

[2] V. Venkatachalam, S. Ganapathy, I. Perumal, and M. Anandhan, "Crystal shape and size of CdTe colloidal quantum dots controlled by silver doping for enhanced quantum dots sensitized solar cells performance," *Colloids Surfaces A Physicochem. Eng. Asp.*, vol. 656, pp. 130–296, Jan. 2023, doi: 10.1016/j.colsurfa.2022.130296.

[3] P. Yang, F. Dong, Y. Yu, J. Shi, and M. Sun, "Copper ion detection method based on a quantum dot fluorescent probe," *Mater. Sci.*, vol. 28, no. 2, pp. 138–143, May 2022, doi: 10.5755/j02.ms.28024.

[4] Pooja and P. Chowdhury, "Functionalized CdTe fluorescence nanosensor for the sensitive detection of water borne environmentally hazardous metal ions," *Opt. Mater.*, vol. 111, p. 110584, Jan. 2021, doi: 10.1016/j.optmat.2020.110584.

[5] M. Kumar *et al.*, "Peptide- and drug-functionalized fluorescent quantum dots for enhanced cell internalization and bacterial debilitation," *ACS Appl. Bio Mater.*, vol. 3, no. 4, pp. 1913–1923, Apr. 2020, doi: 10.1021/acsabm.9b01074.

[6] V. Venkatachalam, S. Ganapathy, T. Subramani, and I. Perumal, "Aqueous CdTe colloidal quantum dots for bio-imaging of Artemia sp," *Inorg. Chem. Commun.*, vol. 128, p. 108510, Jun. 2021, doi: 10.1016/j.inoche.2021.108510.

[7] J. S. Kamal *et al.*, "Size-dependent optical properties of zinc blende cadmium telluride quantum dots," *J. Phys. Chem. C*, vol. 116, no. 8, pp. 5049–5054, Mar. 2012, doi: 10.1021/jp212281m.

[8] N. T. Hien *et al.*, "Synthesis, characterization and the photoinduced electron-transfer energetics of CdTe/CdSe type-II core/shell quantum dots," *J. Lumin.*, vol. 217, p. 116822, Jan. 2020, doi: 10.1016/j.jlumin.2019.116822.

[9] Y. Cao *et al.*, "Xylenol orange-modified CdTe quantum dots as a fluorescent/colorimetric dual-modal probe for anthrax biomarker based on competitive coordination," *Talanta*, vol. 261, p. 124664, Aug. 2023, doi: 10.1016/j.talanta.2023.124664.

[10] J. Hou *et al.*, "Efficient detection of formaldehyde by fluorescence switching sensor based on GSH-CdTe," *Microchem. J.*, vol. 190, p. 108647, Jul. 2023, doi: 10.1016/j.microc.2023.108647.

[11] D. Qi, H. Zhang, Z. Zhou, and Z. Ren, "Preparation of CdTe quantum dots for detecting Cu(II) ions," *Opt. Mater.*, vol. 142, p. 114048, Aug. 2023, doi: 10.1016/j.optmat.2023.114048.

[12] X. Zhu, Z. Zhao, X. Chi, and J. Gao, "Facile, sensitive, and ratiometric detection of mercuric ions using GSH-capped semiconductor quantum dots," *Analyst*, vol. 138, no. 11, p. 3230, Jan. 2013, doi: 10.1039/c3an00011g.

[13] H. Li *et al.*, "Silver ion-doped CdTe quantum dots as fluorescent probe for Hg 2+ detection," *RSC Adv.*, vol. 10, no. 64, pp. 38965–38973, Jan. 2020, doi: 10.1039/d0ra07140d.

[14] Q. B. Hoang *et al.*, "Size-dependent reactivity of highly photoluminescent CdZnTeS alloyed quantum dots to mercury and lead ions," *Chem. Phys.*, vol. 552, p. 111378, Jan. 2022, doi: 10.1016/j.chemphys.2021.111378.

[15] C. L. Hartley, M. L. Kessler, and J. L. Dempsey, "Molecular-level insight into semiconductor nanocrystal surfaces," *J. Am. Chem. Soc.*, vol. 143, no. 3, pp. 1251–1266, Jan. 2021, doi: 10.1021/jacs.0c10658.

[16] Z. Xiaoyong *et al.*, "(Yb3+, Mn2+) Co-doped CdTe nanocrystals with enhanced quantum yields and red-shift emission," *J. Indian Chem. Soc.*, vol. 99, no. 9, p. 100651, Sep. 2022, doi: 10.1016/j.jics.2022.100651.

[17] O. V. Chashchikhin and M. F. Budyka, "Photoactivation, photobleaching and photoetching of CdS quantum dots − Role of oxygen and solvent," *J. Photochem. Photobiol. A Chem.*, vol. 343, pp. 72–76, Jun. 2017, doi: 10.1016/j.jphotochem.2017.04.028.

[18] B. Hosnedlova *et al.*, "Study of physico-chemical changes of cdte qds after their exposure to environmental conditions," *Nanomaterials*, vol. 10, no. 5, p. 865, Apr. 2020, doi: 10.3390/nano10050865.

[19] J. Wang, B. Yang, X. Yu, S. Chen, W. Li, and X. Hong, "The impact of Zn doping on CdTe quantum dots-protein corona formation and the subsequent toxicity at the molecular and cellular level," *Chem. Biol. Interact.*, vol. 373, p. 110370, Mar. 2023, doi: 10.1016/j.cbi.2023.110370.

[20] H. Wang *et al.*, "Enhanced stability and emission intensity of aqueous CdTe/CdS core–shell quantum dots with widely tunable wavelength," *Can. J. Phys.*, vol. 92, no. 7/8, pp. 802–805, Jul. 2014, doi: 10.1139/cjp-2013-0557.

[21] Y. Jiang *et al.*, "Ultrafast synthesis of near-infrared-emitting aqueous CdTe/CdS quantum dots with high fluorescence," *Mater. Today Chem.*, vol. 20, p. 100447, Jun. 2021, doi: 10.1016/j.mtchem.2021.100447.

[22] N. X. Ca *et al.*, "Photoluminescence properties of CdTe/CdTeSe/CdSe core/alloyed/shell type-II quantum dots," *J. Alloys Compd.*, vol. 787, pp. 823–830, May 2019, doi: 10.1016/j.jallcom.2019.02.139.

[23] J. Du *et al.*, "Microwave-assisted synthesis of highly luminescent glutathione-capped Zn1−xCdxTe alloyed quantum dots with excellent biocompatibility," *J. Mater. Chem.*, vol. 22, no. 22, p. 11390, Jan. 2012, doi: 10.1039/c2jm30882g.

[24] O. Adegoke and E. Y. Park, "Size-confined fixed-composition and composition-dependent engineered band gap alloying induces different internal structures in L-cysteine-capped alloyed quaternary CdZnTeS quantum dots," *Sci. Rep.*, vol. 6, no. 1, p. 27288, Jun. 2016, doi: 10.1038/srep27288.

[25] W. Li, J. Liu, K. Sun, H. Dou, and K. Tao, "Highly fluorescent water soluble CdxZn1−xTe alloyed quantum dots prepared in aqueous solution: one-step synthesis and the alloy effect of Zn," *J. Mater. Chem.*, vol. 20, no. 11, p. 2133, Jan. 2010, doi: 10.1039/b921686c.

[26] Q. Wang, T. Fang, P. Liu, B. Deng, X. Min, and X. Li, "Direct synthesis of high-quality water-soluble CdTe:Zn 2+ quantum dots," *Inorg. Chem.*, vol. 51, no. 17, pp. 9208–9213, Sep. 2012, doi: 10.1021/ic300473u.

[27] C. R. S. Matos, L. P. M. Candido, H. O. Souza, L. P. da Costa, E. M. Sussuchi, and I. F. Gimenez, "Study of the aqueous synthesis, optical and electrochemical characterization of alloyed ZnxCd1-xTe nanocrystals," *Mater. Chem. Phys.*, vol. 178, pp. 104–111, Aug. 2016, doi: 10.1016/j.matchemphys.2016.04.076.

[28] H. Q. Bac, V. A. Duc, N. T. Nhan, N. V. Hao, N. V. Quang, and M. X. Dung, "Unexpected photoluminescence enhancement of red-emitting cdte quantum dots by Cu2+ ions," *TNU J. Sci. Technol.*, vol. 227, no. 02, pp. 54–60, Feb. 2022, doi: 10.34238/tnu-jst.5323.

[29] J. Wang *et al.*, "Capillary sensors composed of CdTe quantum dots for real-time in situ detection of Cu 2+," *ACS Appl. Nano Mater.*, vol. 4, no. 9, pp. 8990–8997, Sep. 2021, doi: 10.1021/acsanm.1c01608.

[30] C.-F. Peng, Y.-Y. Zhang, Z.-J. Qian, and Z.-J. Xie, "Fluorescence sensor based on glutathione capped CdTe QDs for detection of Cr 3+ ions in vitamins," *Food Sci. Hum. Wellness*, vol. 7, no. 1, pp. 71–76, Mar. 2018, doi: 10.1016/j.fshw.2017.12.001.

[31] J. Huang *et al.*, "Influence of pH on heavy metal speciation and removal from wastewater using micellar-enhanced ultrafiltration," *Chemosphere*, vol. 173, pp. 199–206, Apr. 2017, doi: 10.1016/j.chemosphere.2016.12.137.

[32] X. Li *et al.*, "Cation/Anion exchange reactions toward the syntheses of upgraded nanostructures: principles and applications," *Matter*, vol. 2, no. 3, pp. 554–586, Mar. 2020, doi: 10.1016/j.matt.2019.12.024.